# Spatiotemporal analysis of water area annual variations using a Landsat time series: a case study of nine plateau lakes in Yunnan province, China

Penghai Wu, Huanfeng Shen, Ning Cai, Chao Zeng, Yanlan Wu, Biao Wang & Yan Wang

Published online: 10 Nov 2016.

Submit your article to this journal

Article views: 83

View related articles

View Crossmark data

Taylor & Francis
Taylor & Francis Group

# Spatiotemporal analysis of water area annual variations using a Landsat time series: a case study of nine plateau lakes in Yunnan province, China

Penghai Wu[a,b], Huanfeng Shen[c], Ning Cai[a], Chao Zeng[d], Yanlan Wu[a,b], Biao Wang[a,b] and Yan Wang[e]

[a]School of Resources and Environmental Engineering, Anhui University, Hefei, China; [b]Engineering Center for Geographic Information of Anhui province, Hefei, China; [c]School of Resource and Environmental Sciences, Wuhan University, Wuhan, China; [d]State Key Laboratory of Hydroscience and Engineering, Tsinghua University, Beijing, China; [e]Key Laboratory of Watershed Geographic Sciences, Chinese Academy of Sciences, Nanjing, China

## ABSTRACT

Lakes are sensitive to both climate change and human activities, and therefore serve as an excellent indicator of environmental change. Based on a time series of Landsat images over the last 16 years, this article attempts to provide a first picture of the annual variations in area of nine plateau lakes in Yunnan province, China. The modified normalized difference water index (MNDWI) and object-based image analysis (OBIA) are used to extract the waterbodies. Compared with the visual interpretation (VI) of the lakes, the precision of the combined method is greater than 99.7%. A spatiotemporal analysis is also carried out for the lakes. The results show that the water areas of most of the plateau lakes have been stable over the last 16 years, although some years have shown significant changes. However, it should be noted that Lake Qilu and Lake Yilong shrunk significantly after 2011. Moreover, the orientation of the shrinkage is different. Limited evidence suggests that the differences in the area change of the nine plateau lakes are caused by both climate change and human activities.

## 1. Introduction

Lakes are multifunctional natural resources and, as an important component of the terrestrial hydrosphere, they provide domestic water, production water, and rich biological resources. The area change of lakes can be caused by both climate change and anthropogenic activities, making lakes significant indicators of regional response or even global drivers (Ma et al. 2011, 2010; Li et al. 2015; Huang et al. 2016). The plateau lakes in the Yunnan province of southwestern China also play an important supporting role in social and economic development, especially ecotourism. However, with the intensification of climate change and human activities in Yunnan, the plateau lake areas have decreased, and the problem of ecological environment deterioration has drawn wide

---

attention (Whitmore et al. 1997; Wang et al. 2012). Therefore, monitoring of the lakes in Yunnan province is required to provide important information for regional development, the utilization and protection of the lakes, and to reveal the impact of human activity and climate change.

The remote-sensing technique, which can provide large-scale water surface information, has been proved to have unique advantages in the dynamic monitoring of large lakes (Zhang et al. 2011). Waterbodies have been mapped and detected using optical and radar imagery over the past few decades (Song, Huang, and Ke 2013). Images from the Advanced Very High Resolution Radiometer (AHVRR) (Barton and Bathols 1989), the Satellite Pour l'Observation de la Terre (SPOT) (Davranche, Lefebvre, and Poulin 2010), Landsat (Frazier and Page 2000), the Advanced Spaceborne Thermal Emission and Reflection Radiometer (ASTER) (Sivanpillai and Miller 2010), and the China-Brazil Earth Resources Satellite (CBERS) (Song et al. 2014) have been used successfully for waterbody identification and monitoring. Among these satellites or sensors, the Landsat series are the most widely used because of the high spatial resolution (30 m), free access, and the 30 years of data records (Hansen et al. 2014; Feyisa et al. 2014; Jiang et al. 2014; Mueller et al. 2016; Du et al. 2012). Numerous methods have been proposed to extract water-bodies from Landsat images. There are three common categories of methods: spectral analysis, supervised and unsupervised classification, and water indices (Jiang et al. 2014). Although a number of water extraction techniques have been described in the literature, the choice among them is constrained by accuracy problems (Feyisa et al. 2014). Of the above-mentioned methods, water indices have been widely used because of their relatively high accuracy in waterbody detection and their low-cost implementation (Jiang et al. 2014; Feyisa et al. 2014), especially the normalized difference water index (NDWI) (McFeeters 1996) and the modified NDWI (MNDWI) (Xu 2006). For instance, Ji, Zhang, and Wylie (2009) aimed to identify the best method among four different water indices for delineating the water features using simulated data sets of different satellite sensors (Ji, Zhang, and Wylie 2009). Among their four alternatives, they found that the MNDWI performed the best in delineating water, and featured the most stable threshold, which was consistent with the conclusions of other studies (Zhai et al. 2015; Sun et al. 2012). Although the MNDWI method can effectively identify waterbodies, our target here is strictly lakes, not other waterbodies. Further identification is therefore required. In addition, most of the existing studies have mainly focused on the monitoring of area changes in lakes using Landsat images of different time periods, but not images from the same season in consecutive years (Rokni et al. 2014; Zhang et al. 2011), so they cannot provide accurate data on the annual variations of lakes.

The objectives of the present case study are: (1) to generate a database from Landsat series sensors of nine plateau lakes in Yunnan province, China, which have been observed during the dry season over the last 16 years; (2) to identify the water features of the nine plateau lakes using the MNDWI and OBIA); and (3) to provide a spatiotemporal analysis of the water area annual variations of these lakes with the Landsat time series. Our objective is to provide the first comprehensive picture of the changes of the nine plateau lakes over the last 16 years, which could be used to examine how climate change and human activities might have affected the nine plateau lakes in Yunnan province, China.

## 2. Materials and methods

### 2.1. Study area

The nine major plateau lakes in the study area are Lake Lugu, Lake Chenghai, Lake Erhai, Lake Dianchi, Lake Yangzonghai, Lake Fuxian, Lake Qilu, Lake Xingyun, and Lake Yilong. The region of the nine plateau lakes (see Figure 1), which is located in SW China's Yunnan province between 21°29′ N–29°19′ N and 97°50′ E–105°36′ E, has a range of elevation from 6,740 m in the northwest to 76 m in the southeast, with an average
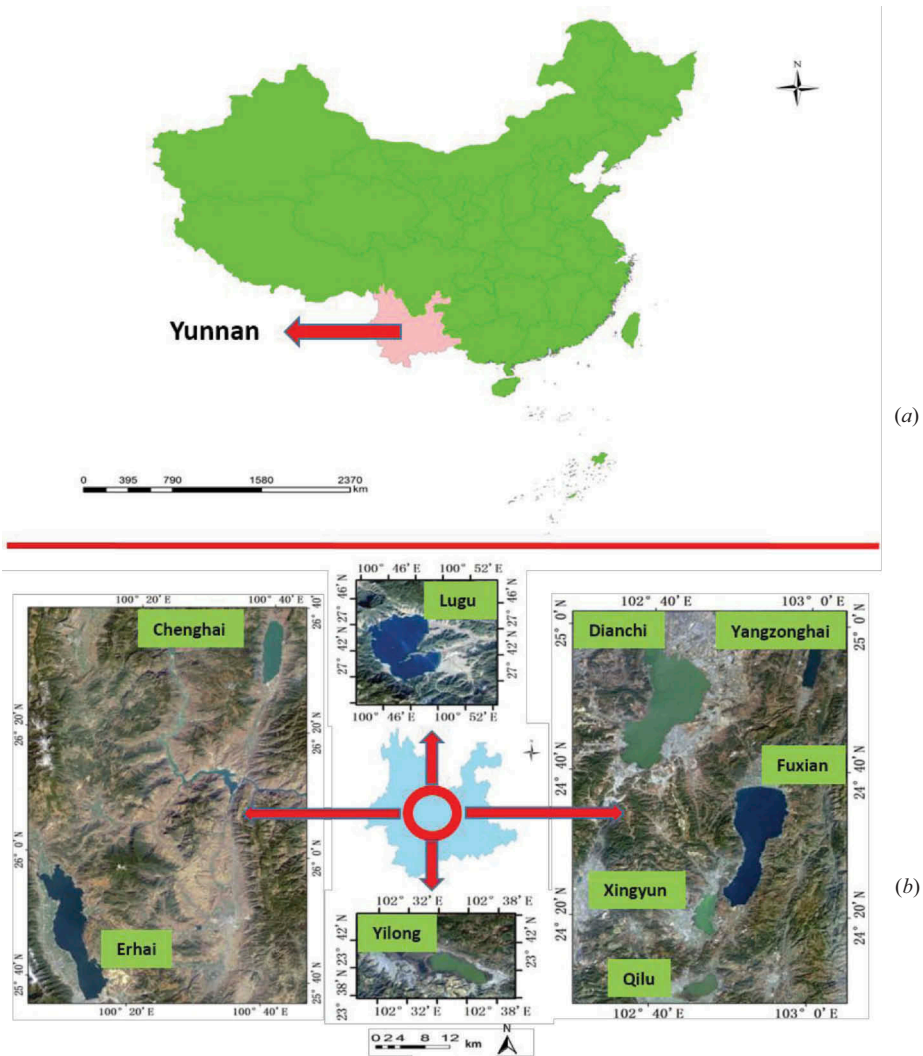


**Figure 1.** The study area and location of the nine plateau lakes in China. The region of the nine plateau lakes is located in SW China's Yunnan province a), and distributed in four Landsat images with different path/row locations (b). The different path/row locations and their contained lakes are listed in Table 2.

elevation of around 2,000 m (Yang et al. 2005). The region has a distinctive monsoon climate with an annual mean temperature of about 15☐ and an annual mean precipitation of over 1,000 mm (Yang et al. 2005). The dry and wet seasons are distinctly separate in Yunnan, and around 90% of the annual precipitation is concentrated in the rainy season (May–October) (Liu et al. 2007). The region containing the lakes in Yunnan Plateau has been designated as a Global 200 Priority Ecoregion of the Palearctic Lake Ecosystems (Olson and Dinerstein 1998), and has attracted considerable attention. The nine plateau lakes belong to the five prefectures of Kunming, Yuxi, Dali, Lijiang, and Honghe, and they are connected to the Changjiang River, the Zhujiang River, and the Lancang River.

## 2.2. *Landsat data*

The Landsat images used in this case study consist of Thematic Mapper (TM) images of Landsat 5, Enhanced Thematic Mapper Plus (ETM+) images of Landsat 7, and OLI images of Landsat 8. The details of the band range and resolution of the OLI sensor and the TM/ETM+ sensor are shown in Table 1. The similar band range and resolution can ensure data consistency for this case study. We use all of the available Level 1 T Landsat TM/ETM+/OLI images from 2000 to 2015 with a cloud cover of less than 5% in this case study, which were downloaded from the United States Geological Survey (USGS) (http://glovis.usgs.gov) or the International Scientific & Technical Data Mirror Site, the Computer Network Information Center, Chinese Academy of Sciences (http://www.gscloud.cn). Owing to the nine plateau lakes being located with wide spatial ranges over the Yunnan province, a total of 64 images from four locations (Path 129, Row 43; Path 129, Row 44; Path 131, Row 41; Path 131, Row 42) were used (see Table 2). To reduce the influence of rainfall, all the images were selected from January to March (see Table 2). The downloaded Landsat images (L1T product) provide systematic radiometric and geometric accuracy by incorporating ground control points, while employing a digital elevation model for topographic accuracy (Shen et al. 2013). More details of the currently available L1T data can be found online (Wulder et al. 2012). To reduce the atmospheric effects, the digital number values of each image are converted to units of surface reflectance using the Fast Line-of-sight Atmospheric Analysis of Spectral Hypercubes (FLAASH) model (Nazeer, Nichol, and Yung 2014).

**Table 1.** The details of the band range and resolution of the OLI sensor and the TM/ETM+ sensor.

| | OLI | | | | TM/ETM+ | | |
|---|---|---|---|---|---|---|---|
| No. | Band | Range (nm) | Resolution (m) | No. | Band | Range (nm) | Resolution (m) |
| 1 | Deep blue | 433–453 | 30 | 1 | Blue | 450–515 | 30 |
| 2 | Blue | 450–515 | 30 | 2 | Green | 525–605 | 30 |
| 3 | Green | 525–600 | 30 | 3 | Red | 630–690 | 30 |
| 4 | Red | 630–680 | 30 | 4 | NIR | 775–900 | 30 |
| 5 | NIR | 845–885 | 30 | 5 | MIR | 1550–1750 | 30 |
| 6 | SWIR1 | 1560–1660 | 30 | 6 | TIRS | 10400–12500 | 30 |
| 7 | SWIR2 | 2100–2300 | 30 | 7 | MIR | 2080–2350 | 30 |
| 8 | Pan | 500–680 | 15 | 8 | Pan (ETM+) | 520–900 | 15 |
| 9 | Cirrus | 1360–1390 | 30 | | | | |

**Table 2.** The Landsat data used to extract the waterbodies.

| Path/row | Contained lakes | Sensors | Date |
|---|---|---|---|
| 129/43 | Dianchi, Xingyun, Qilu, Fuxian Yangzonghai | TM | 28 February 2003, 10 March 2004, 26 February 2005, 24 March 2009, 7 February 2010, 10 February 2011 |
| | | ETM+ | 20 February 2000, 2 March 2001, 9 February 2002, 19 January 2006, 23 February 2007, 9 January 2008, 5 February 2012, 7 February 2013 |
| | | OLI | 2 February 2014, 4 January 2015 |
| 129/44 | Yilong | TM | 10 March 2004, 26 February 2005, 8 March 2009, 7 February 2010, 10 February 2011 |
| | | ETM+ | 20 February 2000, 6 January 2001, 9 February 2002, 28 February 2003, 3 January 2006, 23 February 2007, 29 March 2008, 20 January 2012, 7 February 2013 |
| | | OLI | 2 February 2014, 4 January 2015 |
| 131/41 | Lugu | TM | 9 January 2000, 15 February 2002, 4 January 2004, 6 January 2005, 25 January 2006, 1 March 2007, 16 February 2008, 2 February 2009, 8 February 2011 |
| | | ETM+ | 4 February 2001, 25 January 2003, 28 January 2010, 3 February 2012, 5 February 2013 |
| | | OLI | 31 January 2014, 2 January 2015 |
| 131/42 | Chenghai, Erhai | TM | 1 January 2000, 14 January 2002, 5 February 2004, 6 January 2005, 25 January 2006, 1 March 2007, 16 February 2008, 2 February 2009, 8 February 2011 |
| | | ETM+ | 3 January 2001, 25 January 2003, 28 January 2010, 3 February 2012, 5 February 2013 |
| | | OLI | 31 January 2014, 3 February 2015 |

The dates of the SLC-off images are marked in red.

## 3. Methodology

### 3.1. *Generation of the database covering the dry season over the last 16 years*

Since the scan line corrector (SLC) of the Landsat ETM+ sensor failed permanently in May 2003, only in the centre of the image (of approximately 22 km wide) do the scans give near-contiguous coverage of the surface scanned below the satellite (Maxwell 2004). To differentiate the degraded data, the images acquired before the SLC failure are designated as 'SLC-on' images, and those acquired after the SLC failure are designated as 'SLC-off' images (Zeng, Shen, and Zhang 2013). Landsat 5 TM stopped acquiring images in November 2011, and the data are sparse in the regions with no local receiver, whereas the Landsat 8 OLI started recording images in March 2013 (Wulder et al. 2012). Gap filling in the SLC-off ETM+ images is therefore necessary to ensure the continuity of this satellite observation series. Among the many gap-filling methods that have been proposed in the literature, the multi-temporal methods have proved effective for the Landsat ETM+ gaps (Zeng, Shen, and Zhang 2013). In this case study, we used 16 SLC-off images (marked in Table 2 in the red font), and the missing pixels were recovered using a free plug-in that was recently developed at Wuhan University, which is called the multi-temporal weighted linear regression (WRL) and regularization algorithm (Zeng, Shen, and Zhang 2013).

For convenience, an SLC-off image to be restored is defined as the primary image, whereas an auxiliary image is referred to as the fill image. An un-scanned pixel in the gaps of the primary image is defined as a target pixel, and the respective location is

named the target location. For each missing target pixel, the linear relationship hypothesis is represented as follows:

$$Y = a \times X + b, \tag{1}$$

where $Y$ and $X$ are the pixels at the target location in the primary image and another temporal auxiliary image, respectively, and $a$ and $b$ are the regression coefficients calculated in a local search window using similar pixels. An adaptive determination procedure for the search window and similar pixels can be found in that reference (Zeng, Shen, and Zhang 2013).

Owing to the different degrees of gap overlapping, two or more auxiliary images are needed in a multi-temporal recovery procedure. However, it is often the case that the available images are not sufficient to fill all the missing pixels because the gaps cannot be completely covered. In this case, it is necessary to recover the remaining pixels using a regularization-based recovery method (Zeng, Shen, and Zhang 2013).

## 3.2. *Estimation of the water areas of the lakes*

To enhance the water features with large amounts of built-up land in the background, Xu (2006) proposed the MNDWI, in which the mid-infrared (MIR) band and the green band are used. The MNDWI can be expressed as follows:

$$\text{MNDVI} = (R_{\text{Green}} - R_{\text{MIR}})/(R_{\text{Green}} + R_{\text{MIR}}), \tag{2}$$

where $R_{\text{Green}}$ is the reflectance value of the green band such as Landsat TM/ETM+ band 2, and $R_{\text{MIR}}$ is the reflectance value of the MIR band such as Landsat TM/ETM+ band 5, whereas the green band is band 3 and the MIR band is band 6 for Landsat OLI.

The MNDWI can be used to extract waterbodies effectively such as lakes, rivers, and reservoirs. However, this case study is only concerned with the nine plateau lakes. Accordingly, a further identification is required to ensure the accuracy of the water area. OBIA (or geospatial OBIA (GEOBIA)), which emulates the ability of a human interpreter, has been used as an automatic interpretation method since the late 1990s (Schiewe, Tufte, and Ehlers 2001). The OBIA approach involves two main steps: segmentation and classification (Sun et al. 2012). Image segmentation incorporates the spectral, geometric (e.g. shape, size), texture, and topographic features to group similar image pixels into image objects or homogeneous geo-objects (Benz and Schreier 2001). For instance, Van der Werff and Van der Meer (2008) took into account the shape measures of image objects, such as the compactness, roundness, and convexity, to classify rivers, lakes, and reservoirs in Landsat imagery (Van der Werff and Van der Meer 2008).

For the OBIA approach, there are two main parameters that must be carefully set. The first main parameter is named the scale parameter, and it is a threshold that controls the degree of heterogeneity within an image object. A higher scale parameter leads to larger and less-homogeneous objects, and vice versa. The scale parameter was set from 35 to 45 in this study. The second main parameter is named the feature parameter, and it consists of spectral, texture, and spatial features. Owing to the fact that the water areas of the target lakes are much bigger than the areas of other waterbodies in our study area, the spatial area is sufficient. The feature parameter changes with the target lake, and is usually set as half the area of the target lake. In this case study, we performed a

number of trial-and-error attempts with the two main parameters, until the resulting objects closely correspond to the boundaries of the landscape features. After operating the workflows of MNDWI and OBIA, the target lakes can be segmented as nine independent objects, and we can then calculate the water pixels and their areas.

## 4. Results

### 4.1. *Error analysis of the gap-filling method with different auxiliary images*

Auxiliary images are critical in the multi-temporal recovery procedure. An explanation of how to select the auxiliary images should therefore be given. Two series of experiments (EXP1 and EXP2) were carried out. In EXP1, we considered the SLC-off image observed on 5 February 2012 (path 129, row 43) as the primary image. The additional download image observed on 20 January 2012 and the existing image observed on 7 February 2013 were used as the auxiliary images. The recovery results are listed in Figure 2. Figure 2(a) is the filled image obtained using the auxiliary image observed on 7 February 2013, and Figure 2(b) is the filled image obtained using the auxiliary image observed on 20 January 2012. Figure 2(c,d) are the detailed regions cropped from (*a*) and (*b*), respectively. From Figure 2(c,d), we can see that the auxiliary images have little effect on the recovery result. However, the sharpness is much better preserved in the detailed region cropped from (*b*) than in that cropped from (*a*). The most likely reason for this is that the auxiliary image observed on 20 January 2012 has more similar observational conditions to the primary image (5 February 2012) than another auxiliary image (7 February 2013).

To test the error in the lake area extraction using different auxiliary images, the gap-filled images were used to extract the lake area based on MNDWI+OBIA. The extracted results are shown in Figure 3. Figure 3(a,b) are the extracted results obtained using the gap-filled images in Figure 2(a,b), respectively. From a visual inspection, there are no distinct differences between Figure 3(a,b). Quantitative values of the lake areas in
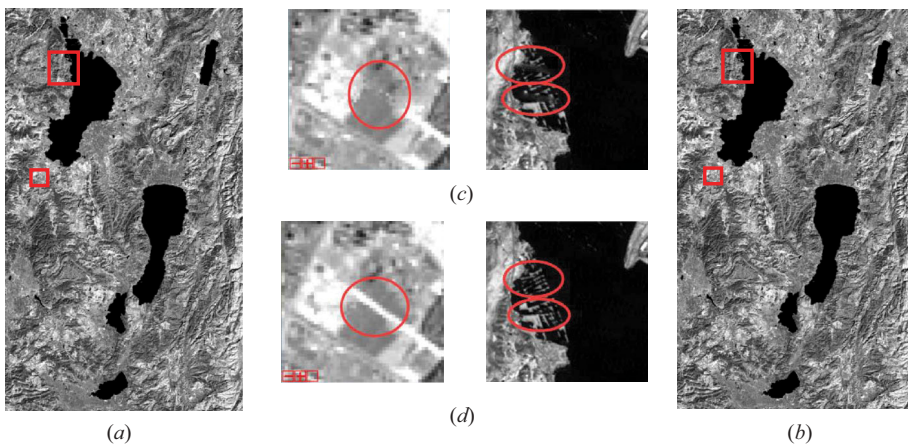


**Figure 2.** The filled results for EXP1. (a) Filled image (5 February 2012) obtained using auxiliary image (7 February 2013). (b) Filled image (5 February 2012) obtained using auxiliary image (20 January 2012). (c) Detailed regions cropped from (a). (d) Detailed regions cropped from (b).

(a) (b)
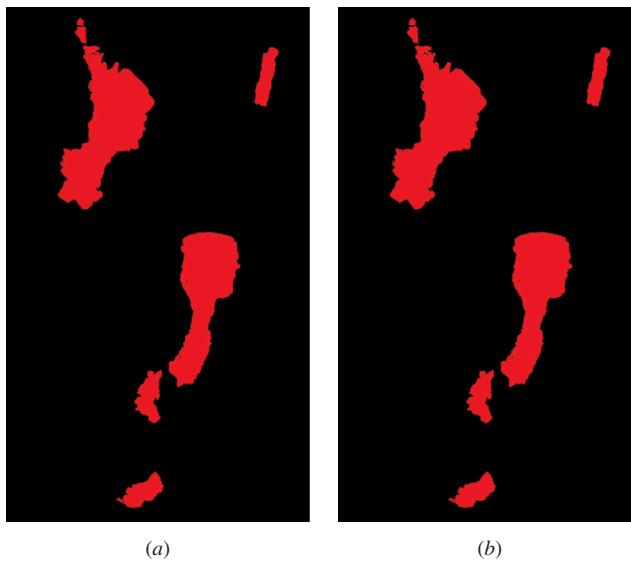
**Figure 3.** The extracted results for EXP1. (a) The extracted result using the filled image in Figure 2(a). (b) The extracted result using the filled image in Figure 2(b).

**Table 3.** Statistics of the water areas (km$^2$) of the results in EXP1.

| Lake | Dianchi | Yangzonghai | Fuxian | Xingyun | Qilu | Sum |
|------|---------|-------------|--------|---------|------|-----|
| Figure 3(a) area: | 281.19 | 29.42 | 213.88 | 33.6 | 32.16 | 590.25 |
| Figure 3(b) area: | 281.6 | 29.39 | 213.9 | 33.55 | 31.95 | 590.39 |
| Difference: | −0.41 | 0.03 | −0.02 | 0.05 | 0.21 | −0.14 |

Figure 3(a,b) are shown in Table 3, where it can be seen that the extracted areas are very similar. The maximum error for the five lakes between Figure 3(a,b) is less than 0.41 km$^2$, and the total error (Sum) is −0.14 km$^2$. Therefore, in this study, there is no significant difference when using the auxiliary image observed on 20 January 2012 and the image observed on 7 February 2013.

Moreover, similar experiments (EXP2) were carried out on the SLC-off image observed on 19 January 2006 and the auxiliary images observed on 8 March 2006 and 3 February 2007 (Path 129, Row 43). Quantitative values of the lake areas are listed in Table 4. The same conclusion as EXP1 can be drawn from Table 4: the extracted results are similar when using the auxiliary image observed on 8 March 2006 and the image observed on 3 February 2007. These experiments verify the authors' opinion that, with multi-temporal auxiliary data, the proposed gap-filling method can restore the invalid pixels accurately, even when obvious changes take place (Zeng, Shen, and Zhang 2013).

**Table 4.** Statistics of the water areas (km$^2$) of the results in EXP2.

| Lake | Dianchi | Yangzonghai | Fuxian | Xingyun | Qilu | Sum |
|------|---------|-------------|--------|---------|------|-----|
| Using the auxiliary image observed on 3 February 2007: | 312.95 | 31.39 | 217.38 | 37.59 | 35.69 | 635 |
| Using the auxiliary image observed on 8 March 2006: | 313.17 | 31.42 | 217.51 | 37.69 | 35.74 | 635.53 |
| Difference: | −0.22 | −0.03 | −0.13 | −0.1 | −0.05 | −0.53 |

**Table 5.** The primary and auxiliary images for the recovery method used in this study.

| Path/row | Images | Date |
|---|---|---|
| 129/43 | Primary images | 19 January 2006, 23 February 2007, 9 January 2008, 5 February 2012, 7 February 2013 |
| | Auxiliary images | 23 February 2007, 9 January 2008, 23 February 2007, 7 February 2013, 5 February 2012 |
| 129/44 | Primary images Auxiliary images | 3 January 2006, 23 February 2007, 29 March 2008, 20 January 2012, 7 February 2013 |
| | | 23 February 2007, 29 March 2008, 23 February 2007, 7 February 2013, 20 January 2012 |
| 131/41 | Primary images Auxiliary images | 28 January 2010, 3 February 2012, 5 February 2013 |
| | | 3 February 2012, 5 February 2013, 3 February 2012 |
| 131/42 | Primary images Auxiliary images | 28 January 2010, 3 February 2012, 5 February 2013 |
| | | 3 February 2012, 28 January 2010, 3 February 2012 |

In this study, the SLC-off images and the corresponding auxiliary images for the gap-filling method are listed in Table 5.

## 4.2. Precision validation of the water extraction method

In this section, we consider the image (Path 129, Row 43) observed on 7 February 2010 as an example to validate the precision of the water extraction method. The reasons for the choice of image are: (1) it contains five of the nine lakes (Lake Dianchi, Lake Yangzonghai, Lake Fuxian, Lake Xingyun, and Lake Qilu); (2) it belongs to high-quality data; and 3) we should consider a Landsat TM image as our example because most of the images in this study are obtained from the TM sensor. Because we are lacking official statistical data, visual interpretation (VI) was carried out in ArcGIS 10.0 as the 'real' standard data to assess the performance of the MNDWI +OBIA method. The qualitative and quantitative results are listed in Figure 4 and Table 6. The extracted waterbodies are quite consistent with the VI result for all of



(a)  (b)  (c)
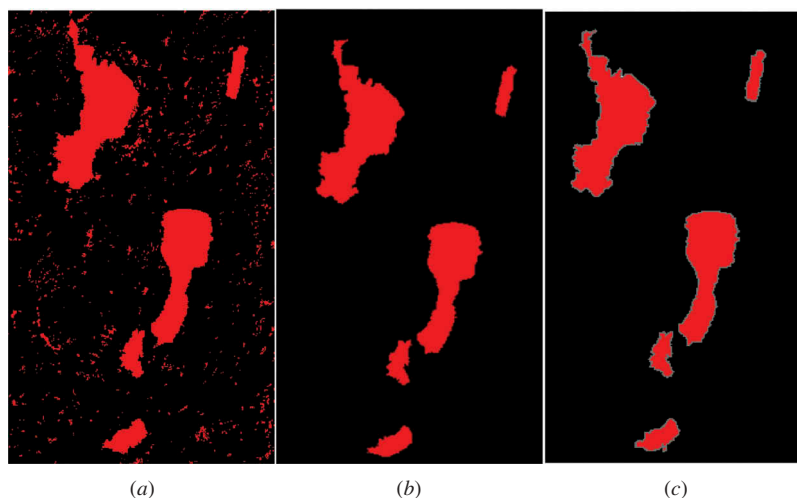
**Figure 4.** Comparison of the lake area extraction using different methods: (a) MNDWI; (b) MNDWI +OBIA; and (c) visual interpretation.

**Table 6.** Accuracy comparison of the lake areas extracted by the proposed method and visual interpretation for the image from 2010.

| Lake | MNDWI+ OBIA(km$^2$) | VI (km$^2$) | Precision (%) |
| --- | --- | --- | --- |
| Dianchi | 295.24 | 295.88 | 99.78 |
| Yangzong | 29.80 | 29.82 | 99.92 |
| Fuxian | 214.21 | 214.85 | 99.70 |
| Xingyun | 33.68 | 33.24 | 98.70 |
| Qilu | 35.94 | 36.01 | 99.54 |

the five lakes shown in Figure 4. Although the pixels of the extracted waterbodies are either slightly more or less in number than those from VI, the precision is greater than 99.7% for all five lakes shown in Table 6.

## 4.3. Spatiotemporal change of the lake area

By means of MNDWI+OBIA, the water pixels of the nine plateau lakes over the last 16 years were calculated. Since one pixel in a Landsat image covers 900 m$^2$ (the spatial resolution is 30 m), the areas of the different lakes in each year were also computed. The largest lake is Lake Dianchi, and the smallest lake is Lake Yilong. Most of the lakes have an area of less than 100 km$^2$, except for Lake Erhai, Lake Dianchi, and Lake Fuxian.

To illustrate the change of the lake areas over time intuitively, we convert the statistical data of the nine plateau lakes into line graphs. According to the area sizes and the magnitude of the changes, the change trends of the lakes are shown in Figure 5. The change of three lakes (Dianchi, Erhai, and Fuxian) with area >200 km$^2$ is depicted in Figure 5(a). The differences in their areas between 2000 and 2015 are small, although some years show significant changes. The changes in Lake Dianchi are of a greater magnitude than the changes in Lake Erhai and Lake Fuxian. In Figure 5(b), the four lakes
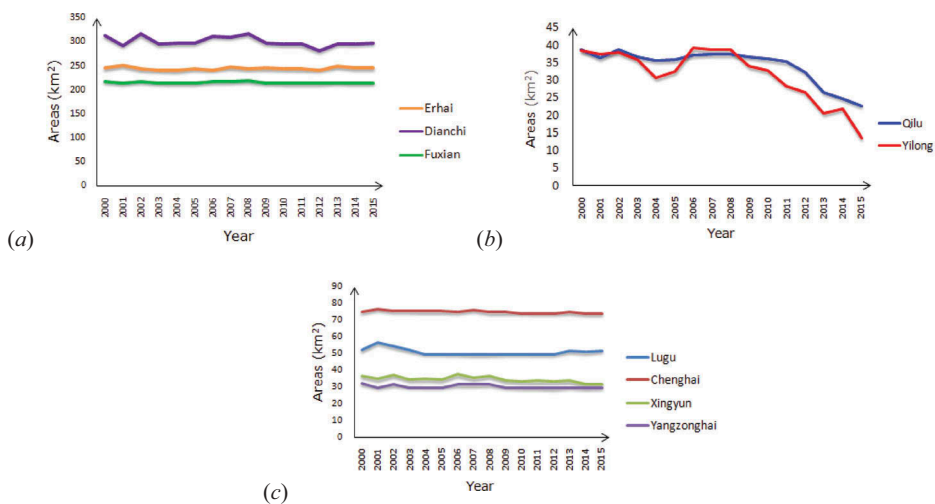


**Figure 5.** The change trends of the areas of the nine plateau lakes from 2000 to 2015: (a) Lake Erhai, Lake Dianchi, and Lake Fuxian; (b) Lake Lugu, Lake Chenghai, Lake Xingyun, and Lake Yangzonghai; and (c) Lake Qilu and Lake Yilong.

**Table 7.** The reduced areas (km$^2$) of Lake Qilu and Lake Yilong in each orientation during the different periods.

| Lake | Time | N | NE | E | SE | S | SW | W | NW |
|------|------|---|----|----|----|----|----|----|----|
| Qilu | 2000–2011 | 0.28 | 0.35 | 0.31 | 0.37 | 0.48 | 0.61 | **1.04** | 0.11 |
| | 2011–2013 | 0.099 | 0.56 | 0.25 | 0.18 | 0.86 | **5.56** | 1.09 | 0.095 |
| | 2013–2015 | 0.20 | −0.0045 | 0.02 | 0.18 | 0.32 | **1.93** | 1.13 | 0.054 |
| | 2000–2015 | 0.58 | 0.90 | 0.58 | 0.74 | 1.66 | **8.10** | 3.27 | 0.26 |
| Yilong | 2000–2009 | 0.050 | 0.13 | 0.32 | 0.47 | 0.071 | 0.28 | 1.26 | **1.80** |
| | 2009–2012 | 0.24 | 0.17 | 0.71 | 0.62 | 0.26 | 0.18 | 2.35 | **2.81** |
| | 2012–2015 | 0.22 | 0.25 | 0.51 | 0.34 | 0.17 | 0.17 | **10.14** | 1.16 |
| | 2000–2015 | 0.51 | 0.55 | 1.54 | 1.43 | 0.50 | 0.63 | **13.75** | 5.77 |

N: north; NE: northeast; E: east; SE: southeast; S: south; SW: southwest; W: west; NW: northwest.
The biggest reduced areas of Lake Qilu and Lake Yilong in certain orientation during the different periods are bolded.

(Lugu, Chenghai, Xingyun, and Yangzonghai) with area in the range 30–80 km$^2$ are shown. The greatest amplitude of variation is <5 km$^2$ for all four lakes from 2000 to 2015. However, Lake Qilu and Lake Yilong significantly decreased in area, which is clearly shown in Figure 5(c). The area of Lake Qilu in 2015 was less than half that in 2000, while the area of Lake Yilong in 2015 was only about one-third of that in 2000. Moreover, unlike Lake Qilu, which has continually shrunk in size, the area of Lake Yilong increased in some years.

The shrinking of the lake areas can be embodied not only in time but also in space, which is closely related to the geographical location and local climate conditions. For Lake Qilu and Lake Yilong, there were different directions of shrinkage during different periods. It is therefore necessary to analyse the orientation of the shrinkage for these two lakes. Table 7 lists the reduced areas of Lake Qilu and Lake Yilong in each orientation during the different periods. The west of Lake Qilu was the main area of shrinkage (1.04 km$^2$) during 2000–2011, whereas the serious shrinkage (5.56 km$^2$) occurred in the southwest of the lake during 2011–2013. From 2013 to 2015, the southwest of Lake Qilu was again the main area of shrinkage (1.93 km$^2$). For Lake Yilong, the northwest of the lake was the main area of shrinkage (1.80 + 2.81 km$^2$) during 2000–2012, and the serious shrinkage (10.14 km$^2$) occurred in the west of the lake during a short interval (from 2012 to 2015). From Table 6, we can see that: (1) the west of Lake Yilong is the main area of shrinkage, whereas the southwest of Lake Qilu is the main area of shrinkage; (2) the area of shrinkage in the west of Lake Yilong (13.75 km$^2$) is about 56% of the total area of shrinkage (24.68 km$^2$), whereas the area of shrinkage in the southwest of Lake Qilu (8.10 km$^2$) is about 50% of the total area of shrinkage (16.10 km$^2$); and (3) from 2012 to 2013, Lake Qilu and Lake Yilong show the greatest degree of shrinkage, with up to 18% and 23%, respectively.

Owing to the fact that Lake Qilu and Lake Yilong reduced at an alarming rate after 2010, we provide thematic maps of the waterbodies in Figure 6. The six colours represent the lake areas in the different periods. Figure 6 shows the area and orientation of the shrinkage for the two lakes, which are in accordance with the foregoing analysis.

## 5. Discussion

The nine plateau lakes in Yunnan province, China, play an important role in supporting urban development, modern agricultural development, tourism, and so on. However,
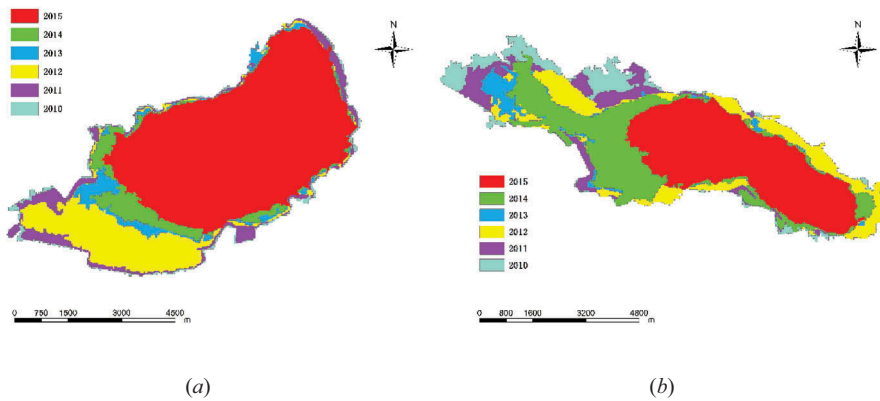
**Figure 6.** The borders of the waterbodies from 2010 to 2015: (a) Lake Qilu, and (b) Lake Yilong.

some of the lakes are facing a serious threat from shrinkage caused by climate change and human activities. To better protect and manage these lakes, it is necessary to monitor the area of the lakes using remote-sensing observations over a long timescale. The Landsat TM/ETM+/OLI images with a 30 m spatial resolution that were used in this study were recorded during the dry season (from January to March) over the last 16 years. For the ETM+ SLC-off images, a gap-filling method called the multi-temporal WRL and regularization algorithm was used. This method can make good use of the multi-temporal information and the spatial information to restore the invalid pixels accurately, even when changes take place (Zeng, Shen, and Zhang 2013). Although these images were all observed during the dry season, errors caused by precipitation (about 10%) still exist. Such errors can be reduced if the images used are acquired in the same month or even on the same day every year. The recent popularity of spatiotemporal fusion (Shen et al. 2013; Wu et al. 2013, 2015), which involves blending different types of satellite images (such as Landsat and Moderate Resolution Imaging Spectroradiometer (MODIS)) to generate synthesized data with both a high spatial resolution and frequent coverage, may provide a solution (Gao et al. 2006).

To extract waterbodies from Landsat images effectively, the adopted MNDWI is regarded as an effective method, although numerous other water index methods have also been proposed. The MNDWI is suitable for enhancing and extracting water information for a region with a background dominated by built-up areas (Xu 2006). Since the water information may consist of rivers, lakes, and reservoirs in Landsat imagery, a further identification of lakes should be carried out. Our experience with the nine plateau lakes suggests that the area-based feature extraction method can correctly identify lakes because of the water areas of the target lakes being much bigger than those of the other sources. It should be noted that although the water extraction technique is extremely important for this study, it is out of the scope of this study. However, the water extraction method (MNDWI+OBIA) was adopted based on a great deal of literature and experiments.

As global warming intensifies, China is facing an increasing drought risk in the twenty-first century under the changing climate (Xu et al. 2015). Drought is becoming

more and more serious in SW China's Yunnan province (Huang et al. 2015). A period of continuous drought in Yunnan province from 2009 to 2014 was reported in several studies (Zhang et al. 2015), which may have played an important role in reducing precipitation and affecting lake changes. To support our analysis, data gathered from 36 meteorological stations all over Yunnan province from 2000 to 2013 (data after 2013 are not yet available) were downloaded from the China Meteorological Administration (http://data.cma.cn/). First, the mean annual temperature (MAT) and the mean annual rainfall (MAR) were calculated, as shown in Table 8. In general, the MAT shows a rising tendency whereas the MAR shows a decreasing trend from 2000 to 2013. The highest MAT occurred in 2010, and the lowest MAR occurred in 2009. The Yunnan Meteorological Service stated that the 15 years from 2000 to 2014 were the lowest MAR period on record in Yunnan province. These data suggest that Yunnan province is suffering from high MAT and light MAR under global climate warming, which might have played an important role in the lake changes.

The statistical results of the nine plateau lakes between 2000 and 2015 showed that most of the lakes have shrunk to a small degree, except for Lake Qilu and Lake Yilong. The intriguing point is that the area change of Lake Qilu and Lake Yilong showed a slowly decreasing trend in the first decade, whereas the speed of area decline was faster in the last five years (especially in 2013). The influencing factors were not only continuous drought, but also some human activities (Wu, Déry, and Wu 2015). For instance, reclamation of the lakes and the construction of the Trans-Asian Railway directly affected the water resource balance of Lake Qilu (Zhang and Nie 2013), whereas urban expansion, field irrigation, and a blocked water supply caused the shrinkage of Lake Yilong (Wang 2015). Furthermore, most of the productive farmland and the Yu-Meng section of the Trans-Asian Railway are located to the west and southwest of Lake Qilu, which is consistent with its main area of shrinkage. For Lake Yilong, land reclamation from the lake has been used for the urban expansion of Shiping County. The west of Lake Yilong was the main area of shrinkage because Shiping County locates to the west and the northwest of the lake. Moreover, the potential reason for the areas of the other lakes being relatively stable is that most of them are important tourism destinations and are replenished throughout the year. Lake Dianchi is a typical example, where water from Niulan Jiang is transferred into Lake Dianchi to maintain the water level (Li and Xiao 2015). Overall, the driving factors for area change of the nine plateau lakes are relatively complicated. However, we want to emphasize that the difference in the area change among the nine plateau lakes is the result of human activities and climate change.

In this case study, we generated a 16 consecutive year database at the Landsat scale for the nine plateau lakes in Yunnan province, China, which were observed during the dry season. These data were used to reveal the water area annual variations (both size and

**Table 8.** The mean annual temperature (MAT) and the mean annual rainfall (MAR) from 2000 to 2013 in Yunnan province.

| Content | Upper rows: 2000–2007; lower rows: 2008–2013 | | | | | | |
|---|---|---|---|---|---|---|---|
| MAT (°C) | 16.5 | 16.9 | 16.9 | 17.2 | 16.6 | 17.2 | 17.2 | 16.8 |
| | 16.6 | 17.4 | 17.6 | 16.8 | 17.4 | 17.3 | | |
| MAR (mm) | 1139.6 | 1241.1 | 1137.1 | 937.8 | 1113.3 | 1032.1 | 996.7 | 1133.3 |
| | 1164.7 | 848.9 | 1029.3 | 853.9 | 926.6 | 1006.8 | | |

direction) over a long timescale. However, it should be noted that there is room for improvement for the methods used in this case study. First, the spatial resolution of the Landsat multi-spectral images is 30 m, and mixed pixels often occur in the lake boundaries. As a result, errors in the statistical results are inevitable. The theory of the decomposition of mixed pixels could help improve this situation (Michishita, Gong, and Xu 2012; Ma et al. 2014). Second, due to the fact that we are lacking official statistical data, VI was used to assess the water extraction method. However, validation of the precision is still in our future research agenda. In addition, we did not provide a comparison of the surface water extraction performances of the other methods (not water indices). The MNDWI was applied to all nine plateau lakes, but it might not have been the best method for all the lakes.

## 6. Conclusions

In this case study, we generated a database from a Landsat time series of the nine plateau lakes in Yunnan province, China, which were observed during the dry season over the last 16 years. The waterbodies of the lakes were identified successfully using the MNDWI and OBIA, and the results were consistent with those of the VI. Although the sensors of the Landsat series of satellites are different, the experimental results provide comprehensive long-term information about lake changes for the same spatial scale in Yunnan province, China. The results will also allow a better understanding of the effect of climate change and human activity on the nine lakes in the Yunnan Plateau. The results of the spatiotemporal analysis suggest that the differences in the area change among the nine plateau lakes are caused by climate change and human activities. Although the case study only used the nine plateau lakes as an example, it has opened up a new avenue for other lakes in the world. Such a capability will be beneficial for the monitoring and management of water resources, and to reveal the impact of human activity and climate change.

# References

Barton, I. J., and J. M. Bathols. 1989. "Monitoring Floods with AVHRR." *Remote Sensing of Environment* 30 (1): 89–94. doi:10.1016/0034-4257(89)90050-3.

Benz, U., and G. Schreier. 2001. "Definiens Imaging GmbH: Object Oriented Classification and Feature Detection." *IEEE Geoscience and Remote Sensing Society Newsletter* 9: 16–20.

Davranche, A., G. Lefebvre, and B. Poulin. 2010. "Wetland Monitoring Using Classification Trees and SPOT-5 Seasonal Time Series." *Remote Sensing of Environment* 114 (3): 552–562. doi:10.1016/j.rse.2009.10.009.

Du, Z., B. Linghu, F. Ling, W. Li, W. Tian, H. Wang, Y. Gui, B. Sun, and X. Zhang. 2012. "Estimating Surface Water Area Changes Using Time-Series Landsat Data in the Qingjiang River Basin, China." *Journal of Applied Remote Sensing* 6 (1): 063609. doi:10.1117/1.JRS.6.063609.

Feyisa, G. L., H. Meilby, R. Fensholt, and S. R. Proud. 2014. "Automated Water Extraction Index: A New Technique for Surface Water Mapping Using Landsat Imagery." *Remote Sensing of Environment* 140: 23–35. doi:10.1016/j.rse.2013.08.029.

Frazier, P. S., and K. J. Page. 2000. "Water Body Detection and Delineation with Landsat TM Data." *Photogrammetric Engineering and Remote Sensing* 66 (12): 1461–1468.

Gao, F., J. Masek, M. Schwaller, and F. Hall. 2006. "On the Blending of the Landsat and MODIS Surface Reflectance: Predicting Daily Landsat Surface Reflectance." *IEEE Transactions on Geoscience and Remote Sensing* 44 (8): 2207–2218. doi:10.1109/TGRS.2006.872081.

Hansen, M., A. Egorov, P. Potapov, S. Stehman, A. Tyukavina, S. Turubanova, D. Roy, S. Goetz, T. Loveland, and J. Ju. 2014. "Monitoring Conterminous United States (CONUS) Land Cover Change with Web-Enabled Landsat Data (WELD)." *Remote Sensing of Environment* 140: 466–484. doi:10.1016/j.rse.2013.08.014.

Huang, L., X. Xu, J. Zhai, and C. Sun. 2016. "Local Background Climate Determining the Dynamics of Plateau Lakes in China." *Regional Environmental Change* 1–14. doi:10.1007/s10113-016-0963-x.

Huang, Y., C. Xu, H. Yang, J. Wang, D. Jiang, and C. Zhao. 2015. "Temporal and Spatial Variability of Droughts in Southwest China from 1961 to 2012." *Sustainability* 7 (10): 13597–13609. doi:10.3390/su71013597.

Ji, L., L. Zhang, and B. Wylie. 2009. "Analysis of Dynamic Thresholds for the Normalized Difference Water Index." *Photogrammetric Engineering & Remote Sensing* 75 (11): 1307–1317. doi:10.14358/PERS.75.11.1307.

Jiang, H., M. Feng, Y. Zhu, N. Lu, J. Huang, and T. Xiao. 2014. "An Automated Method for Extracting Rivers and Lakes from Landsat Imagery." *Remote Sensing* 6 (6): 5067–5089. doi:10.3390/rs6065067.

Li, L., and M. Xiao. 2015. "Study on Implicit Composite Element Method for Seepage Analysis in Underground Engineering." *Science China Technological Sciences* 58 (10): 1617–1626. doi:10.1007/s11431-015-5888-y.

Li, Q., L. Lu, C. Wang, Y. Li, Y. Sui, and H. Guo. 2015. "MODIS-Derived Spatiotemporal Changes of Major Lake Surface Areas in Arid Xinjiang, China, 2000–2014." *Water* 7 (10): 5731–5751. doi:10.3390/w7105731.

Liu, Y., E. Zhao, W. Huang, Y. Zhu, and Y. Tao. 2007. "General Circulation Characteristic Before Beginning of Yunnan Rainy Season." *Journal of Arid Meteorology* 25 (3): 17–22.

Ma, B., L. Wu, X. Zhang, X. Li, Y. Liu, and S. Wang. 2014. "Locally Adaptive Unmixing Method for Lake-Water Area Extraction Based on MODIS 250m Bands." *International Journal of Applied Earth Observation and Geoinformation* 33: 109–118. doi:10.1016/j.jag.2014.05.002.

Ma, R., H. Duan, C. Hu, X. Feng, A. Li, W. Ju, J. Jiang, and G. Yang. 2010. "A Half-Century of Changes in China's Lakes: Global Warming or Human Influence?" *Geophysical Research Letters* 37 (24): L24106. doi:10.1029/2010GL045514.

Ma, R., G. Yang, H. Duan, J. Jiang, S. Wang, X. Feng, A. Li, F. Kong, B. Xue, and J. Wu. 2011. "China's Lakes at Present: Number, Area and Spatial Distribution." *Science China Earth Sciences* 54 (2): 283–289. doi:10.1007/s11430-010-4052-6.

Maxwell, S. 2004. "Filling Landsat ETM+ SLC-Off Gaps Using a Segmentation Model Approach." *Photogrammetric Engineering and Remote Sensing* 70 (10): 1109–1112.

McFeeters, S. 1996. "The Use of the Normalized Difference Water Index (NDWI) in the Delineation of Open Water Features." *International Journal of Remote Sensing* 17 (7): 1425–1432. doi:10.1080/01431169608948714.

Michishita, R., P. Gong, and B. Xu. 2012. "Spectral Mixture Analysis for Bi-Sensor Wetland Mapping Using Landsat TM and Terra MODIS Data." *International Journal of Remote Sensing* 33 (11): 3373–3401. doi:10.1080/01431161.2011.611185.

Mueller, N., A. Lewis, D. Roberts, S. Ring, R. Melrose, J. Sixsmith, L. Lymburner, A. McIntyre, P. Tan, and S. Curnow. 2016. "Water Observations from Space: Mapping Surface Water from 25years of Landsat Imagery across Australia." *Remote Sensing of Environment* 174: 341–352. doi:10.1016/j.rse.2015.11.003.

Nazeer, M., J. E. Nichol, and Y.-K. Yung. 2014. "Evaluation of Atmospheric Correction Models and Landsat Surface Reflectance Product in an Urban Coastal Environment." *International Journal of Remote Sensing* 35 (16): 6271–6291. doi:10.1080/01431161.2014.951742.

Olson, D. M., and E. Dinerstein. 1998. "The Global 200: A Representation Approach to Conserving the Earth's Most Biologically Valuable Ecoregions." *Conservation Biology* 12 (3): 502–515. doi:10.1046/j.1523-1739.1998.012003502.x.

Rokni, K., A. Ahmad, A. Selamat, and S. Hazini. 2014. "Water Feature Extraction and Change Detection Using Multitemporal Landsat Imagery." *Remote Sensing* 6 (5): 4173–4189. doi:10.3390/rs6054173.

Schiewe, J., L. Tufte, and M. Ehlers. 2001. "Potential and Problems of Multi-Scale Segmentation Methods in Remote Sensing." *GeoBIT/GIS* 6 (01): 34–39.

Shen, H., P. Wu, Y. Liu, T. Ai, Y. Wang, and X. Liu. 2013. "A Spatial and Temporal Reflectance Fusion Model considering Sensor Observation Differences." *International Journal of Remote Sensing* 34 (12): 4367–4383. doi:10.1080/01431161.2013.777488.

Sivanpillai, R., and S. N. Miller. 2010. "Improvements in Mapping Water Bodies Using ASTER Data." *Ecological Informatics* 5 (1): 73–78. doi:10.1016/j.ecoinf.2009.09.013.

Song, C., B. Huang, and L. Ke. 2013. "Modeling and Analysis of Lake Water Storage Changes on the Tibetan Plateau Using Multi-Mission Satellite Data." *Remote Sensing of Environment* 135: 25–35. doi:10.1016/j.rse.2013.03.013.

Song, C., B. Huang, L. Ke, and K. S. Richards. 2014. "Remote Sensing of Alpine Lake Water Environment Changes on the Tibetan Plateau and Surroundings: A Review." *ISPRS Journal of Photogrammetry and Remote Sensing* 92: 26–37. doi:10.1016/j.isprsjprs.2014.03.001.

Sun, F., W. Sun, J. Chen, and P. Gong. 2012. "Comparison and Improvement of Methods for Identifying Waterbodies in Remotely Sensed Imagery." *International Journal of Remote Sensing* 33 (21): 6854–6875. doi:10.1080/01431161.2012.692829.

Van der Werff, H., and F. Van der Meer. 2008. "Shape-Based Classification of Spectrally Identical Objects." *ISPRS Journal of Photogrammetry and Remote Sensing* 63 (2): 251–258. doi:10.1016/j.isprsjprs.2007.09.007.

Wang, J. 2015. "Study on the Living Envirnoment of Ecological Sensitivity Evaluation and Space Optimization in Plateau Lake Basins–The Yilong Lake as an Example." Master Thesis, in Chinese. Yunnan: Yunnan University.

Wang, R., J. A. Dearing, P. G. Langdon, E. Zhang, X. Yang, V. Dakos, and M. Scheffer. 2012. "Flickering Gives Early Warning Signals of a Critical Transition to a Eutrophic Lake State." *Nature* 492 (7429): 419–422. doi:10.1038/nature11655.

Whitmore, T., M. Brenner, Z. Jiang, J. Curtis, A. Moore, D. Engstrom, and Y. Wu. 1997. "Water Quality and Sediment Geochemistry in Lakes of Yunnan Province, Southern China." *Environmental Geology* 32 (1): 45–55. doi:10.1007/s002540050192.

Wu, C., S. Déry, and W. Wu. 2015. "A Review of Water Resources Utilization and Protection in Southwest China." *Sciences in Cold and Arid Regions* 7 (6): 0736–0746.

Wu, P., H. Shen, T. Ai, and Y. Liu. 2013. "Land-Surface Temperature Retrieval at High Spatial and Temporal Resolutions Based on Multi-Sensor Fusion." *International Journal of Digital Earth* 6: (S1):113-133. doi:10.1080/17538947.2013.783131.

Wu, P., H. Shen, L. Zhang, and F.-M. Göttsche. 2015. "Integrated Fusion of Multi-Scale Polar-Orbiting and Geostationary Satellite Observations for the Mapping of High Spatial and

Temporal Resolution Land Surface Temperature." *Remote Sensing of Environment* 156: 169–181. doi:10.1016/j.rse.2014.09.013.

Wulder, M. A., J. G. Masek, W. B. Cohen, T. R. Loveland, and C. E. Woodcock. 2012. "Opening the Archive: How Free Data Has Enabled the Science and Monitoring Promise of Landsat." *Remote Sensing of Environment* 122: 2–10. doi:10.1016/j.rse.2012.01.010.

Xu, H. 2006. "Modification of Normalised Difference Water Index (NDWI) to Enhance Open Water Features in Remotely Sensed Imagery." *International Journal of Remote Sensing* 27 (14): 3025–3033. doi:10.1080/01431160600589179.

Xu, K., D. Yang, H. Yang, Z. Li, Y. Qin, and Y. Shen. 2015. "Spatio-Temporal Variation of Drought in China during 1961–2012: A Climatic Perspective." *Journal of Hydrology* 526: 253–264. doi:10.1016/j.jhydrol.2014.09.047.

Yang, J., W. Zhang, W. Feng, and Y. Shen. 2005. "Freshwater Testate Amoebae of Nine Yunnan Plateau Lakes, China." *Journal of Freshwater Ecology* 20 (4): 743–750. doi:10.1080/02705060.2005.9664798.

Zeng, C., H. Shen, and L. Zhang. 2013. "Recovering Missing Pixels for Landsat ETM+ SLC-Off Imagery Using Multi-Temporal Regression Analysis and a Regularization Method." *Remote Sensing of Environment* 131: 182–194. doi:10.1016/j.rse.2012.12.012.

Zhai, K., X. Wu, Y. Qin, and P. Du. 2015. "Comparison of Surface Water Extraction Performances of Different Classic Water Indices Using OLI and TM Imageries in Different Situations." *Geo-spatial Information Science* 18 (1): 32–42. doi:10.1080/10095020.2015.1017911.

Zhang, B., Y. Wu, L. Zhu, J. Wang, J. Li, and D. Chen. 2011. "Estimation and Trend Detection of Water Storage at Nam Co Lake, Central Tibetan Plateau." *Journal of Hydrology* 405 (1): 161–170. doi:10.1016/j.jhydrol.2011.05.018.

Zhang, C., and M. Nie. 2013. "Lake Qilu: How to Keep Our Mother River." In *Yunnan Economic Daily*. Yunnan: Yunnan Economic Daily. Editor-in-Chief: Tao Li.

Zhang, X., Y. Zhang, L. Sha, C. Wu, Z. Tan, Q. Song, Y. Liu, and L. Dong. 2015. "Effects of Continuous Drought Stress on Soil Respiration in a Tropical Rainforest in Southwest China." *Plant and Soil* 394 (1–2): 343–353. doi:10.1007/s11104-015-2523-4.